THE ASTROPHYSICAL JOURNAL, 468:469–474, 1996 September 10

GALAXY CLUSTERING AROUND NEARBY LUMINOUS QUASARS[1]

KARL B. FISHER, JOHN N. BAHCALL, AND SOFIA KIRHAKOS
Institute for Advanced Study, School of Natural Sciences, Princeton, NJ 08540
AND
DONALD P. SCHNEIDER
Department of Astronomy and Astrophysics, The Pennsylvania State University, University Park, PA 16802
Received 1996 January 8; accepted 1996 March 21

ABSTRACT

We examine the clustering of galaxies around a sample of 20 luminous low redshift ($z \lesssim 0.30$) quasars observed with the Wide Field Camera-2 on the *Hubble Space Telescope* (*HST*). The *HST* resolution makes possible galaxy identification brighter than $V = 24.5$ and as close as 1″ or 2″ to the quasar. We find a significant enhancement of galaxies within a projected separation of $\lesssim 100\ h^{-1}$ kpc of the quasars. If we model the QSO/galaxy correlation function as a power law with a slope given by the galaxy/galaxy correlation function, we find that the ratio of the QSO/galaxy to galaxy/galaxy correlation functions is 3.8 ± 0.8. The galaxy counts within $r < 15\ h^{-1}$ kpc of the quasars are too high for the density profile to have an appreciable core radius ($\gtrsim 100\ h^{-1}$ kpc). Our results reinforce the idea that low redshift quasars are located preferentially in groups of 10–20 galaxies rather than in rich clusters. We see no significant difference in the clustering amplitudes derived from radio-loud and radio-quiet subsamples.

Subject headings: galaxies: clusters: general — quasars: general — radio continuum: galaxies

1. INTRODUCTION

Over the last two decades, it has been well established that quasars are associated with enhancements in the galaxy distribution. Historically, this provided the first direct observational evidence that quasars were indeed cosmological in origin (Bahcall, Schmidt, & Gunn 1969; Bahcall & Bahcall 1970; Gunn 1971; Stockton 1978). Over the years, considerable evidence has accumulated that low-redshift ($z \lesssim 0.4$) quasars reside in small to moderate groups of galaxies rather than in rich clusters (cf. Hartwick & Schade 1990; Bahcall & Chokshi 1991, and references therein). At higher redshifts, there is a marked difference in the environments of radio-loud and radio-quiet quasars (Yee & Green 1987). At redshifts $z \gtrsim 0.6$, radio-loud quasars are often found in association with rich clusters (Abell richness $R \geq 1$), while radio-quiet quasars appear to remain in smaller groups, or, perhaps, in the outer regions of clusters (Boyle, Shanks, & Yee 1988; Yee 1990).

The galaxy environment around quasars provides many important clues as to what triggers and sustains their central engines. As first suggested by Toomre & Toomre (1972), mergers and interactions of galaxies can provide an efficient mechanism for transporting gas into the inner regions of a galaxy or quasar. There have been attempts to model the interaction/merger rates of ordinary galaxies in order to explain the luminosity function of quasars (De Robertis 1985; Roos 1981b; Carlberg 1990), and the rapid evolution of the merger/interaction rate in clusters with redshift may provide a natural explanation of the strong evolution of clustering observed around radio-loud quasars (Stocke & Perrenod 1981; Roos 1981a). Knowledge of the galaxy environment around quasars is also important for understanding the large-scale distribution of quasars and how it relates to the structure seen in galaxy surveys (Bahcall & Chokshi 1991).

In this paper, we examine the galaxy environment around 20 nearby ($z \lesssim 0.3$) bright quasars observed with the Wide Field and Planetary Camera-2 (WFPC2) of the *Hubble Space Telescope* (*HST*). These fields were imaged as part of an ongoing investigation into the nature of the host environment of quasars (Bahcall, Kirhakos, & Schneider 1994, 1995a, 1995b, 1996a). The exceptional resolution of the *HST* images allows companion galaxies to be detected at very close projected separations, in some cases $r \sim 3\ h^{-1}$ kpc ($\lesssim 2''$), and galaxy/star separation to be performed down to $V \sim 24.5$. The goal of the work presented here is to quantify the excess of galaxies associated with these quasars. The outline of this paper is as follows. A brief description of the quasar sample used in our analysis is given in § 2. In § 3.1, we argue that galaxy counts are inconsistent with being drawn from a uniform background. In § 3.2, we strengthen this conclusion by correcting the counts for the background contamination. We also present the excess galaxy counts above the background in annuli of projected separation. From these counts, we quantify the amplitude of the galaxy clustering around the quasars in § 3.3 in terms of a quasar-galaxy spatial cross-correlation amplitude. We discuss our results and their relation to previous work in § 4.

2. DATA

The sample of objects analyzed in this paper consists of 20 of the intrinsically most luminous ($M_V < -22.9$, for $H_0 = 100$ km s^{-1} Mpc^{-1}, $\Omega_0 = 1$) nearby ($z < 0.30$) radio-quiet and radio-loud quasars selected from the Véron-Cetty & Véron (1991) catalog. Table 1 lists the individual quasars and their redshifts. The quasars span the redshift range $0.086 \leq z \leq 0.29$, with a median redshift of $z_{\rm med} = 0.18$. Details of the observations and the resulting images for 11 of the 20 fields have been presented in Bahcall et al. (1994, 1995a, 1995b); the remaining observations will be presented in Bahcall, Kirhakos, & Schneider (1996b). Six of the

[1] Based on observations with the NASA/ESA *Hubble Space Telescope*, obtained at the Space Telescope Science Institute, which is operated by the Association of Universities for Research in Astronomy, Inc., under NASA contract NAS 5-26555.

TABLE 1

QUASAR SAMPLE

Name	Date	Exp. (s)	M_V	z
PG 0052+251	05 Dec 94	1400	−23.0	0.155
PHL 909	17 Oct 94	1400	−22.9	0.171
NAB 0205+02	26 Oct 94	1400	−23.0	0.155
0316−346	20 Nov 94	1400	−24.5	0.265
PG 0923+201	23 Mar 95	1400	−23.0	0.190
PG 0953+414	03 Feb 94	1100	−24.1	0.239
PKS 1004+13[a]	26 Feb 95	1400	−24.3	0.240
PG 1012+00	25 Feb 95	1400	−23.0	0.185
HE 1029−1401.......	06 Feb 95	1400	−23.2	0.086
PG 1116+215	08 Feb 94	1100	−23.7	0.177
PG 1202+281	08 Feb 94	1100	−23.0	0.165
3C 273[a]	05 Jun 94	1100	−25.7	0.158
PKS 1302−102[a]......	09 Jun 94	1100	−24.6	0.286
PG 1307+085	05 Apr 94	1400	−23.1	0.155
3C 323.1[a]	09 Jun 94	1100	−22.9	0.266
PG 1309+355	26 Mar 95	1400	−23.2	0.184
PG 1402+261	07 Mar 95	1400	−23.0	0.164
PG 1444+407	27 Jun 94	1100	−24.0	0.267
PKS 2135−147[a]......	15 Aug 94	1400	−23.5	0.200
PKS 2349−014[a]......	18 Sep 94	1400	−23.3	0.173

[a] Radio loud.

quasars (see Table 1) are radio-loud, while the remainder are radio-quiet (Kellermann 1989).

Each quasar field was imaged with the WFPC2 through the F606W filter, which is similar but slightly redder than the V bandpass (5940 Å, $\Delta = 1500$ Å). The quasars were positioned within $4'' \pm 1''.2$ of the center of Wide Field Camera CCD 3 (WF3). Simultaneous images were obtained in the adjacent CCD chips 2 and 4 (WF2 and WF4, respectively), which together with WF3 form an "L" shaped image (see Fig. 1). Each chip has 800 × 800 pixels and an image scale of $0''.0996$ pixel^{-1} at the chip's center; this corresponds to spatial resolution of 2.1 h^{-1} kpc

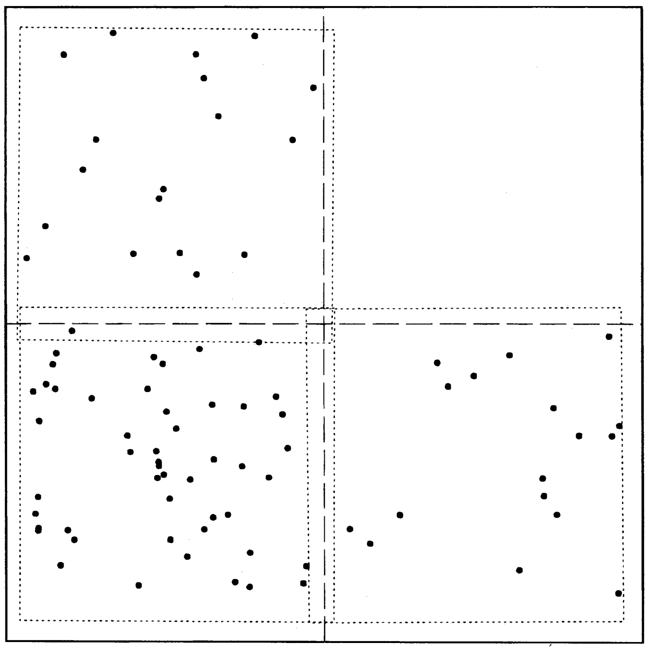

FIG. 1.—Mosaic of the galaxy counts in WF2, WF3, and WF4 (*upper left*, *lower left*, and *right panels*, respectively) for all twenty fields. In a given field i, we count only those galaxies in the magnitude range $m_*(z_i) - 1$ to $m_*(z_i) + 2$, where $m_*(z_i)$ is the apparent magnitude of an L_* galaxy at the redshift of the quasar, z_i.

arcsec^{-1} at a redshift $z = 0.20$ ($\Omega_0 = 1$). The effective areas (areas not covered by pyramid shadows) of WF2, WF3, and WF4 are 1.59, 1.60, and 1.59 arcmin^2, respectively. More detailed information on the WFPC2 and its photometric system can be found in Burrows (1994), Trauger et al. (1994), and Holtzman et al. (1995a, 1995b). The relatively long exposures (1100 or 1400 s), combined with the excellent spatial resolution, allowed galaxies to be identified in the images down to limiting magnitude m(F606W) ≤ 24.5 and as close as $\lesssim 1''$ or $2''$ from the central quasar. We performed aperture photometry on the field galaxies; circular apertures with radii of $0''.3$–$10''$ were used, as appropriate.

3. GALAXY COUNTS AROUND QUASARS

3.1. *Raw Counts*: *Evidence for a Strong Enhancement*

If galaxies are distributed around low-redshift quasars with a power-law distribution, $\xi(r) \sim (r/10\ h^{-1}\ \mathrm{Mpc})^{-1.77}$ (as suggested by, e.g., Yee & Green 1987), then there will be a very strong enhancement of the counts within $30''$ ($r \sim 60$ h^{-1} kpc at $z = 0.2$) of the quasar. Moreover, because the centers of WF2 and WF4 are offset from the quasar, there will be an enhancement of galaxies in WF3 relative to WF2 and WF4. The background galaxy counts rise steeply with magnitude, and this will dilute any signal of excess galaxies. Much of the background contamination can be removed simply by counting only those galaxies with apparent magnitudes in the range that is likely to be physically associated with the quasars. A good compromise between eliminating too many associated galaxies and minimizing the effect of foreground/background interlopers, is to count galaxies in each field, i, that are in the magnitude range $m_*(z_i) - 1$ to $m_*(z_i) + 2$, where $m_*(z_i)$ is the apparent magnitude of an L_* galaxy at the redshift of the quasar, z_i. The mean (median) value of $m_*(z_i)$ for our sample is 18.2 (18.1); the total range of $m_*(z_i)$ is $16.4 \leq m_*(z_i) \leq 19.2$. In computing $m_*(z)$, we have taken an L_* galaxy to correspond to an absolute magnitude $M_*(\mathrm{F606W}) = -20.75$ and have used the K corrections between absolute and apparent magnitudes given in Fukugita, Shimasaku, & Ichikawa (1995).

Figure 1 shows the positions of all galaxies in our twenty fields, with $m_*(z_i) - 1 \leq m \leq m_*(z_i) + 2$; geometric corrections were applied according to Holtzman et al. (1995a). In the panel containing the quasar (WF3, *lower left*), there is a clear excess of galaxies (50 galaxies) relative to WF2 (*upper left*) and WF4 (18 and 17 galaxies, respectively). The hypothesis that the counts in all three chips are drawn from an underlying Poisson distribution with a common mean leads to a maximum likelihood mean per chip of 28.4 and $\chi^2 = 24.5$; the probability that χ^2 for one degree of freedom is this large by chance, is only $P = 7 \times 10^{-7}$. Thus, without any detailed modeling, we can rule out the possibility that the counts are random fluctuations in the background distribution. In the following sections, we attempt to make this conclusion progressively more quantitative, by first modeling the background galaxy distribution, and then introducing a model for the spatial distribution of galaxies around the quasars.

3.2. *Correcting for the Background Galaxies*

In order to further quantify the excess of galaxy counts around the quasars, we need an estimate of the contribution from background galaxies. In Figure 2, we show the galaxy counts ($d^2N/dm\,d\Omega$ arcsec^{-2}) versus magnitude for the

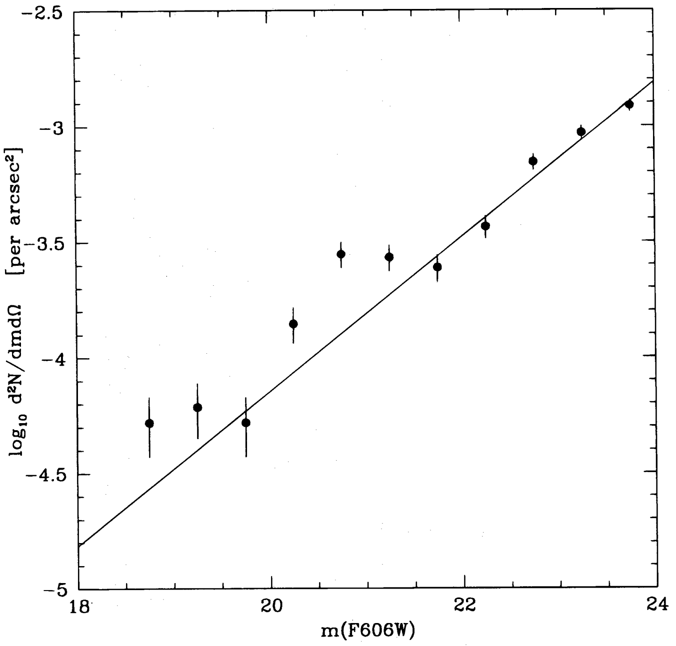

FIG. 2.—Number counts, $d^2N/dm\,d\Omega$, versus m(F606W). Filled circles represent the counts determined directly from the off chips in each QSO field. Poisson errors are shown. The line is a least squares fit to the faint counts, with m(F606W) > 21.5.

"off quasar" chips WF2 and WF4, in bins Δm(F606W) = 0.5. The counts at m(F606W) > 21.5 mag are well approximated by a power law, $\log_{10} d^2N/dm\,d\Omega = -10.8 + 0.33m$(F606W); the counts at brighter magnitudes are in excess of those obtained by extrapolating the faint power-law fit. Because the separation of the centers of chips 2 and 4 is not large (101″ corresponds to 213 h^{-1} kpc at $z = 0.2$), the counts in these chips are a combination of both background galaxies and the (relatively bright) galaxies physically associated with the quasars, and, hence, they yield an overestimate of the true background. We have compared the power-law fit with the counts derived from the *HST* Medium Deep Survey (MDS) (Griffiths et al. 1994; S. Casertano 1995, private communication), which covers a much larger area of the sky. The agreement is good, and in the remainder of this paper, we will adopt the power law in Figure 2 as our estimate of $d^2N/dm\,d\Omega$. The agreement with the MDS is also a useful consistency check for systematic errors in our derived magnitudes.

In the 20 fields, there are 11 galaxies in the range $m_*(z_i) - 1 \leq m \leq m_*(z_i) + 2$ within a projected separation less than 25 h^{-1} kpc of the quasar; the total number expected from the $d^2N/dm\,d\Omega$ power-law relation is only 0.99. The probability of the observed counts being a Poisson realization of the background is extremely small, $P = 8 \times 10^{-9}$, 2 order of magnitudes smaller than our previous estimate, obtained by neglecting the background. This is also a much stronger constraint than the upper limit given in Bahcall et al. (1995a), $P = 2 \times 10^{-2}$, based on eight fields and an (over)estimate of the background obtained from the counts in WF2 and WF4.

We have also computed counts within projected separations of 5 and 10 h^{-1} kpc. In the 20 fields, we find 2/0.039 and 5/0.16 (number/number expected in the background), with $r < 5$ h^{-1} kpc and $r < 10$ h^{-1} kpc, respectively; the corresponding random probabilities are $P = 7 \times 10^{-4}$ and $P = 7 \times 10^{-7}$. There is a suggestive difference in the counts derived from the radio-loud and radio-quiet subsamples. The radio-quiet quasars (14 fields) had 0/0.027 ($P = 0.97$) and 2/0.11 ($P = 5 \times 10^{-3}$) for the 5 and 10 h^{-1} kpc counts; the corresponding numbers for the radio-loud sample (6 fields) were 2/0.012 ($P = 8 \times 10^{-5}$) and 3/0.05 ($P = 2 \times 10^{-5}$).

In Figure 3, we show the fractional excess of galaxies above the background, $\langle \delta N/N(r) \rangle = \langle N_i(r)/N_{b,i}(r) \rangle - 1$, obtained by averaging the counts in the 20 fields in bins of 15 h^{-1} kpc projected separation. Here $N_i(r)$ is the actual count of galaxies with projected separations between $r - \Delta r/2$ and $r + \Delta r/2$ in the ith field, and $N_{b,i}(r)$ is the expected background contribution. Again, we have only considered those galaxies in the apparent magnitude range $m_*(z_i) - 1$ to $m_*(z_i) + 2$.

From Figure 3, we can immediately draw two conclusions: first, there is a significant excess of galaxies within projected separations of $r < h^{-1}$ kpc from the quasars, and second, there appears to be no significant difference in the galaxy counts for the radio-loud and radio-quiet subsamples for 10 h^{-1} kpc $< r <$ 100 h^{-1} kpc. In the next section, we quantify the observed clustering in terms of the spatial quasar/galaxy cross-correlation function.

3.3. *Estimating the Spatial Clustering Amplitude*

A detailed derivation of the relation between angular counts and a spatial distribution of galaxies in terms of a cross-correlation function is given in Longair & Seldner (1979). Briefly, one assumes that the galaxy distribution (above the background) around the quasar is specified by a quasar/galaxy cross-correlation function, $\xi_{qg}(r, z)$. The observed excess in projected separation in the ith field is then obtained by integrating $\xi_{qg}(r, z)$ over the redshift distribution of galaxies $(d\mathcal{N}/dz)_i$ in the apparent magnitude range $[m_*(z_i) - 1 \leq m \leq m_*(z_i) + 2]$,

$$N_i(r)/N_{b,i}(r) - 1 = \frac{\int d\theta\, dz (d\mathcal{N}/dz)_i\, \xi_{qg}(s, z)}{\int d\theta\, dz (d\mathcal{N}/dz)_i} . \quad (1)$$

In this equation, s is the comoving separation between the line of sight, $x(z)$, and the quasar located at coordinate $x(z_i)$; $s^2 = \{(x(z_i) - x(z))^2/G(x(z))\} + x(z)^2\theta^2$; θ is the angle between the line of sight and the quasar; and $G(x)$ is a function that describes the degree of spatial curvature, $G(x) = 1 - (H_0 x/c)^2(\Omega_0 - 1)$ (cf. Peebles 1980, eq. 56.13). The range of integration in θ corresponds to the angles that span the bin of projected separation, i.e., from $(r - \Delta r/2)/d_a(z_i)$ to $(r + \Delta r/2)/d_a(z_i)$, where $d_a(z_i)$ is the angular diameter distance to the quasar.

The redshift distribution $(d\mathcal{N}/dz)_i$ (assuming no galaxies are created or destroyed) is given by

$$\left(\frac{d\mathcal{N}}{dz}\right)_i = \phi(z_i) \frac{dx}{dz} dV , \quad (2)$$

where $\phi(z_i)$ is the integral of the luminosity function over the absolute magnitudes $[M_*(z_i) - 1 \leq M \leq M_*(z_i) + 2]$, corresponding the apparent magnitude range $[m_*(z_i) - 1 \leq m \leq m_*(z_i) + 2]$,

$$\phi(z_i) \equiv \int_{M_*(z_i)-1}^{M_*(z_i)+2} dM \Phi(M) . \quad (3)$$

The cosmological model (Ω_0, Λ, H_0) enters in the above equations implicitly in the volume element, angular dis-

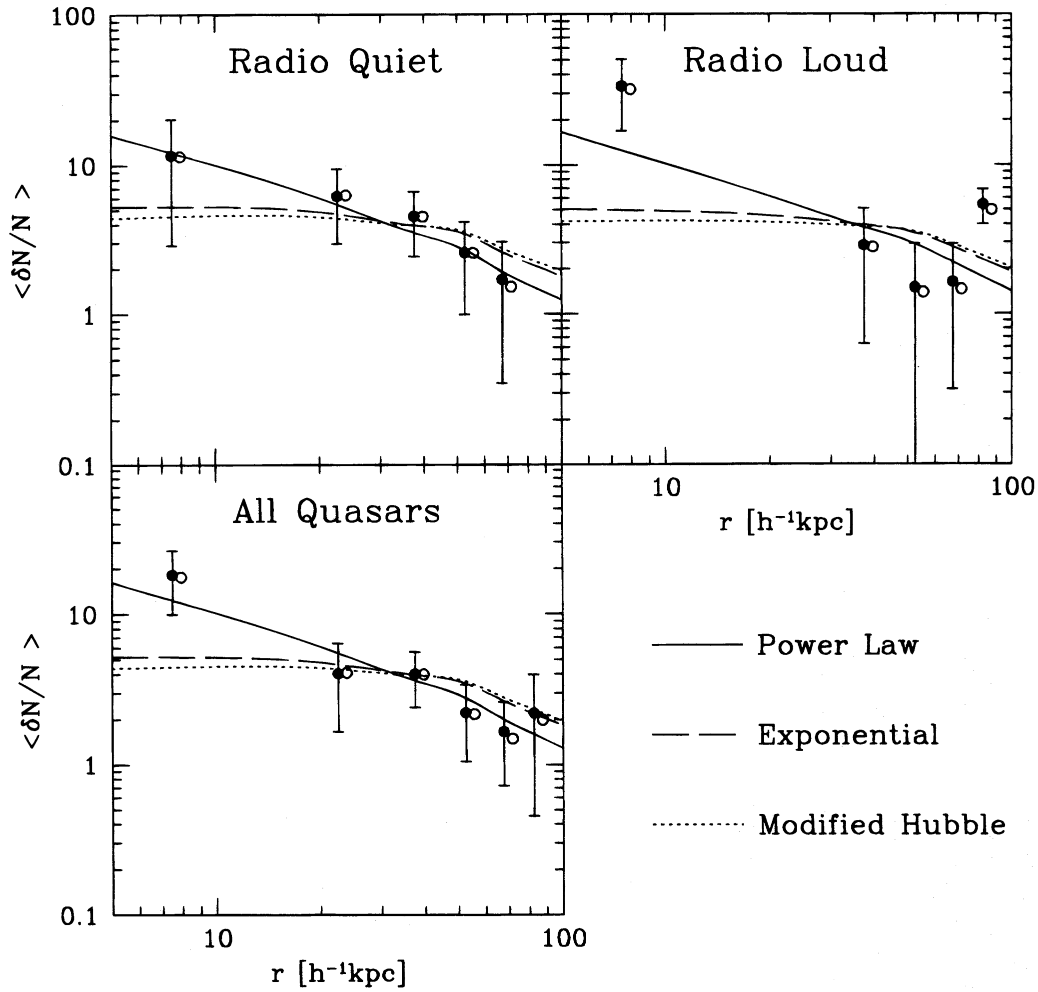

FIG. 3.—Average galaxy counts $\langle \delta N/N(r) \rangle$ of the full quasar sample and radio and radio-quiet subsets. Solid points are the counts computed, using a power-law fit, to the faint counts of chips 2 and 4 for the background (cf. Fig. 2); the open symbols (shifted 0.025 in the log) show the counts derived using the background counts from the Medium Deep Survey. Error bars show the scatter between the different fields. Curves are the predicted correlation functions if the galaxy/quasar cross correlation function is a power law with index $\gamma = 1.77$ (*solid*), an exponential surface density (*dashed*), or a modified Hubble profile (*dotted*). All calculations assume $\Omega_0 = 1$ and $\Lambda = 0$.

tance, and luminosity distance. We adopt a canonical model, with $\Omega_0 = 1$, $H_0 = 100$ km s^{-1} Mpc^{-1}, and $\Lambda = 0$. The basic results of our study are largely independent of this choice. The redshift distribution is computed using a non-evolving Schechter (1976) luminosity function with a faint end slope of $\alpha = 0.97$ (Loveday et al. 1992). The K-corrections necessary for computing the relation between absolute and apparent magnitudes have been taken from Fukugita et al. (1995). In the results that follow, the H_0 dependence is explicitly indicated. The derived clustering amplitudes remain within the stated errors, as Ω_0 is varied from 0.1 to 1.0.

The cross-correlation function, $\xi_{qg}(r, z)$, is usually assumed to evolve with redshift. A convenient model for this evolution is to assume that on small scales the clustering is constant in physical coordinates, i.e., the number of excess galaxies around the quasar, $n(z)\xi_{qg}(r, z)$, is a constant [$n(z)$ is average number density at the epoch z]. Thus, for any assumed shape of the correlation function, $F(r)$, $\xi_{qg}(r, z)$ evolves as

$$\xi_{qg}(r, z) = \frac{1}{(1+z)^3} F\left[\frac{r}{1+z}\right] . \qquad (4)$$

The factor of $(1 + z)^3$ compensates for the change in the mean number density, while the redshift factor in the argument of $F(r)$ is simply a matter of convention; one usually specifies the shape in terms of *physical* separations, while in (1) we have specified $\xi_{qg}(r, z)$ in terms of comoving separation.

We consider three different models for $F(r)$. The first model is a power law, $F(r) = B_{qg} r^{-1.77}$, with a slope equal to that of the galaxy/galaxy correlation function (Davis & Peebles 1983) and the amplitude taken as a free parameter. The second model is an exponential surface density of galaxies, $\mu(r) = \mu_0 \exp(-r/r_c)$, which, after deprojection by a standard Abel inversion, corresponds to $F(r) = \mu_0/\pi r_c K_0(r/r_c)$ ($K_0[x]$ being the modified Bessel function). This model was proposed by Merrifield & Kent (1989) as a typical galaxy profile around centrally dominant cluster galaxies. We adopt their best estimate of a core radius of $r_c = 100\ h^{-1}$ kpc and vary the amplitude μ_0. Finally, we consider a modified Hubble profile $F(r) = A[1 + (r/r_c)^2]^{-3/2}$ (Binney & Tremaine 1987, eqs. 2–37), with $r_c = 100\ h^{-1}$ kpc and A as a free parameter. These three models have different behavior at small r. Both the power-law and exponential models diverge as $r \rightarrow 0$ [although the later

TABLE 2

CLUSTERING AMPLITUDES

Sample	$\langle B_{qg} \rangle$[a]	$1-\sigma$ Range	$\langle B_{qg} \rangle / \langle B_{gg} \rangle$[b]
All quasars	75	60–93	3.8 ± 0.8
Radio loud	84	57–117	4.2 ± 1.5
Radio quiet......	72	53–92	3.6 ± 1.0

[a] In units of $[h^{-1}\ \text{Mpc}]^{1.77}$.
[b] $\langle B_{gg} \rangle = 19.8(h^{-1}\ \text{Mpc})^{1.77}$.

does so only weakly, $K_0(x) \sim -\ln(x)$], while the modified Hubble model asymptotically approaches a constant.

We varied the amplitude of the models in order to achieve a maximum likelihood fit to the excess galaxy counts in bins of projected separation of 15 h^{-1} kpc. The limited number of fields prevented us from varying more than one parameter for each model. Figure 3 shows the resulting best-fit models; the amplitudes of the power-law model are given in Table 2. At separations $r \gtrsim 30\ h^{-1}$ kpc, the excess counts are relatively flat and all three models for the correlation function fit the data. However, the counts in the innermost bin, $r < 15\ h^{-1}$ kpc, lie significantly above the counts at larger separations; the rise in the counts at small radii is particularly striking in the five radio-loud fields. The power law is the only model for $\xi_{qg}(r)$ considered that rises steeply enough to account for this excess.

4. DISCUSSION

If the quasars were distributed like typical galaxies, then the derived value of $\langle B_{qg} \rangle$ would be equal to the amplitude of the galaxy/galaxy correlation function, $\langle B_{gg} \rangle \sim 20$ (Davis & Peebles 1983). A higher value of $\langle B_{qg} \rangle$ suggests that the quasars lie preferentially in regions of above average galaxy density. Following Bahcall & Chokshi (1991), we can convert our values of B_{qg} into an estimate of the typical richness of quasar galaxy environment. Here we define richness as the number of L_* galaxies associated with the quasar; this is given by a simple integral over the correlation function, $N = 4\pi n_* \int \xi_{qg}(r) r^2 dr$, where the limits of integration are $r = 0$–$1.5\ h^{-1}$ Mpc (the traditional Abell radius), and $n_* \approx 1.5 \times 10^{-2}\ h^3\ \text{Mpc}^{-3}$ is the number density of L_* galaxies. Using the values of $\langle B_{qg} \rangle$ in Table 2, we find the quasars typically reside in groups of 16–25 galaxies. These numbers should be compared to the typical richness of Abell clusters, which have 30–49 and 50–79 members for richness classes $R = 0$ and $R = 1$, respectively. Moreover, this estimate is most likely an upper limit, since there is evidence that the galaxy profile around quasars falls off more steeply than $r^{-1.77}$ for $r \gtrsim 0.25\ h^{-1}$ Mpc (Ellingson, Yee, & Green 1991). In order to test the robustness of our results to a steepening of the galaxy profile, we fitted a double power-law model with slope -1.77 for $r \leq 0.25\ h^{-1}$ Mpc and -3 for $r > 0.25\ h^{-1}$ Mpc. The best-fit amplitudes, B_{qg}, for this model increased by about 10% (still well within the quoted 1–σ errors), yet, the number of inferred bright galaxies associated with the quasars decreased to eight, owing to the steeper profile at large separations.

The derived amplitudes, $\langle B_{qg} \rangle$, in the pure power-law case are somewhat larger than the estimates by Yee & Green (1987). They examined the clustering of nine radio-loud and 16 radio-quiet quasars in the redshift range $0.15 < z < 0.30$. On scales of $\sim$20–500 h^{-1} kpc, they estimated $\langle B_{qg} \rangle \approx 60 \pm 20$ and $\langle B_{qg} \rangle \approx 42 \pm 14$ for radio-loud and radio-quiet quasars, respectively. Hayman (1990) derived galaxy counts around low-redshift ($z < 0.3$) quasars from the Palomar Sky Survey prints. He found that the ratio of the quasar/galaxy and galaxy/galaxy angular correlation functions was 3.1 ± 0.6; if the quasars and galaxies have similar selection functions, this translates to an estimate similar to Yee & Green of $\langle B_{qg} \rangle \sim 61 \pm 12$. French & Gunn (1983) analyzed a sample 25 low-redshift quasars ($z \lesssim 0.35$) selected from 1.2 m Palomar Schmidt plates, and they concluded that $\langle B_{qg} \rangle = 25 \pm 12$; they also analyzed the data set of Stockton (1978; 27 quasars with redshifts $z \leq 0.45$ selected from the red Sky Survey prints) and derived, via the same analysis, $B_{qg} = 79 \pm 40$. Our measurements are, with the exception of Yee & Green's value for radio-quiet quasars, consistent within the quoted errors. The slightly higher clustering amplitude we derive for the radio-quiet subsample may be a result of our sample being the subset of the most luminous quasars.

Yee & Green (1987) found that the clustering amplitude of galaxies around radio-loud quasars increased by a factor $\sim$3 between $z \sim 0.4$–0.6, and at $z \sim 0.6$, radio-loud quasars are found in environments as rich as Abell class $R = 1$. Optical quasars do not evolve as rapidly (Boyle et al. 1988), perhaps indicating a different formation scenario. It has been suggested that quasars and active galactic nuclei may be triggered by interactions (e.g., Toomre & Toomre 1972; Stocke & Perrenod 1981; Roos 1981a, Yee 1987). This offers a simple explanation for why the quasars are typically not found in rich clusters at low redshifts; the high-velocity dispersion of such clusters leads to a low-interaction rate.

The *HST* WFPC2 is an excellent instrument for extending the present analysis to fainter, low-redshift, quasars. This extension would improve the counting statistics while also providing information regarding possible correlations of the quasar environment with luminosity. The imaging of moderate redshift quasars ($z \lesssim 0.6$) could be accomplished by *HST* with single orbit exposures. This imaging would provide a more direct comparison with previous ground-based work, and it would increase our knowledge of the evolutionary history of the quasar environment. An increased knowledge of the quasar environment would be useful in using quasar observations to probe large-scale structure at higher redshifts.

We would especially like to thank Stefano Casertano and the members of the Medium Deep Survey for useful comments, and for allowing us to compare our number counts and magnitudes with their measurements. We have also benefited from discussions with Neta Bahcall, Michael Strauss, and Ofer Lahav. We thank the anonymous referee for helpful suggestions. This work was supported in part by NASA contract NAG 5-1618, NASA grant NAGW-4452, and grant GO-5343 from the Space Telescope Science Institute, which is operated by the Association of Universities for Research in Astronomy, Incorporated, under NASA contract NAS 5-26555. K. B. F. acknowledges the support of the National Science Foundation.

REFERENCES

Bahcall, J. N., & Bahcall, N. A. 1970, PASP, 82, 721
Bahcall, J. N., Kirhakos, S., & Schneider, D. P. 1994, ApJ, 435, L11
———. 1995a, ApJ, 450, 486
———. 1995b, ApJ, 454, L175
———. 1996a, ApJ, 457, 557
———. 1996b, in preparation
Bahcall, J. N., Schmidt, M., & Gunn, J. E. 1969, ApJ, 157, L77
Bahcall, N. A., & Chokshi, A. 1991, ApJ, 380, L9
Binney, J., & Tremaine, S. 1987, Galactic Dynamics (Princeton: Princeton Univ. Press)
Boyle, B. J., Shanks, T., & Yee, H. K. C. 1988, in IAU Symp. 130, Large Scale Structures of the Universe, ed. J. Audouze, M.-C. Pelletan, & A. Szalay (Dordrecht: Kluwer), 576
Burrows, C. J. 1994, *Hubble Space Telescope* and Planetary Camera-2 Instrument Handbook, Version 2.0 (Baltimore: Space Telescope Science Institute)
Carlberg, R. G. 1990, ApJ, 350, 505
Davis, M., & Peebles, P. J. E. 1983, ApJ, 267, 465
De Robertis, M. M. 1985, AJ, 90, 998
Ellingson, E., Green, R. F., & Yee, H. K. C. 1991, ApJ, 371, 49
French, H. B., & Gunn, J. E. 1983, ApJ, 269, 29
Fukugita, M., Shimasaku, K., & Ichikawa, T. 1995, PASP, 107, 945
Griffiths, R. E., et al. 1994, ApJ, 437, 67
Gunn, J. E. 1971, ApJ, 164, L113
Hartwick, F. D. A., & Schade, D. 1990, ARA&A, 28, 437
Hayman, P. G. 1990, MNRAS, 265, 358
Holtzman, J. A., et al. 1995a, PASP, 107, 156
———. 1995b, PASP, 107, 1065
Kellermann, K. I., Sramek, R., Schmidt, M., Shaffer, D. B., & Green, R. 1989, AJ, 98, 1195
Longair, M. S., & Seldner, M. 1979, MNRAS, 189, 433
Loveday, J., Peterson, B. A., Efstathiou, G., & Maddox, S. 1992, ApJ, 390, 338
Merrifield, M. R., & Kent, S. M. 1989, AJ, 98, 351
Roos, N. 1981a, A&A, 95, 349
———. 1981b, A&A, 104, 218
Schechter, P. L. 1976, ApJ, 203, 297
Stocke, J. T., & Perrenod, S. C. 1985, ApJ, 245, 375
Stockton, A. 1978, ApJ, 223, 747
Toomre, A., & Toomre, J. 1972, ApJ, 178, 623
Trauger, J. T., et al. 1994, ApJ, 435, L3
Véron-Cetty, M. P., & Véron, P. 1991, ESO Scientific Rep. 10, A Catalog of Quasars and Active Nuclei (Fifth Ed.; Paris: ESO)
Yee, H. K. C. 1987, AJ, 94, 1461
———. 1990, in ASP Conf. Ser. Vol. 10, Evolution of the Universe of Galaxies (San Francisco: Book Crafters, Inc.), 322
Yee, H. K. C., & Green, R. F. 1984, ApJ, 280, 79
———. 1987, ApJ, 319, 28